Resolution and depth of investigation studies of Magnetic Resonance Sounding (MRS) using SVD

Mike Müller, Marian Hertrich, Ugur Yaramanci*

Introduction The question of resolution and depth of investigation for the ill-posed MRS inverse problem has been presented in few different ways. Most of them focused on analysing inversion result either changing modeling parameters [6, 5] or using independent inversion runs [1]. A direct estimation of maximum investigation depth for different loopsizes and resistivity cases can be achieved if the maximum depth is defined as a $\frac{1}{e}$ decreased sensitivity (respectively kernel function) value. All of which listed above are more or less subjective and therefore a objective method of analysing model resolution using singular value decomposition (SVD) is presented. Within this we derive a strong dependency of loopsize, resistivity and resolution for a homogenous half space.

Quantifying resolution, depth penetration and image quality As shown in [3] the MRS forward problem can be described as

$$\begin{aligned} V_R(q) &= \omega_L \int d^3\mathbf{r} \left|\mathbf{M}_N^{(0)}(\mathbf{r})\right| \sin\left(q\mathbf{B}_T^+(\mathbf{r})\right) \\ &\quad \times \mathbf{B}_R^-(\mathbf{r}) \cdot e^{i[\zeta_T(\mathbf{r})+\zeta_R(\mathbf{r})]} \\ &\quad \times \left[\widehat{\mathbf{b}}_R(\mathbf{r}) \cdot \widehat{\mathbf{b}}_T(\mathbf{r}) + i\widehat{\mathbf{B}}_0 \cdot \widehat{\mathbf{b}}_R(\mathbf{r}) \times \widehat{\mathbf{b}}_T(\mathbf{r})\right] \end{aligned} \tag{1}$$

and furthermore summarized to

$$V_R(q) = \int d^3\mathbf{r}\; f(\mathbf{r}) \cdot \mathbf{K}(q,\mathbf{r})$$

where **K** is the kernel or sensitivity function. This means the forward problem of MRS can easily be written as a linear mapping without any kind of linear approximation

$$y = Ax \tag{2}$$

while using mathematical standard descriptions A is the kernel or sensitivity function, x the water content of the subsurface and y the measured signal. Following denotation of [2] singular value decomposition to A can be written as

$$A = U\Lambda V^T = [U_p\; U_0] \begin{bmatrix} \Lambda_p & 0 \\ 0 & 0 \end{bmatrix} \begin{bmatrix} V_p^T \\ V_0^T \end{bmatrix} \tag{3}$$

*Technical University Berlin, Ackerstrasse 71-76, Berlin

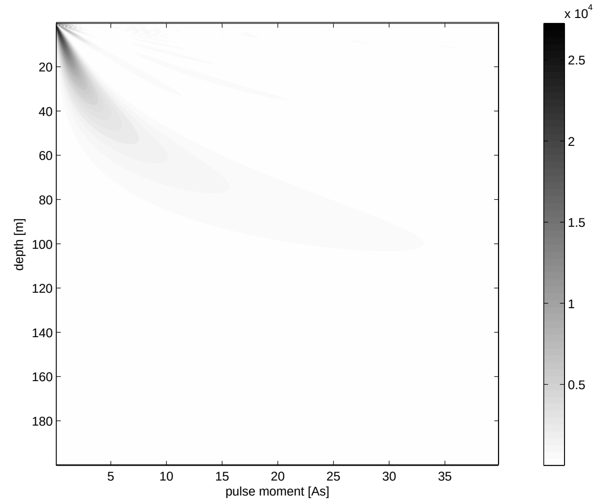

(a)

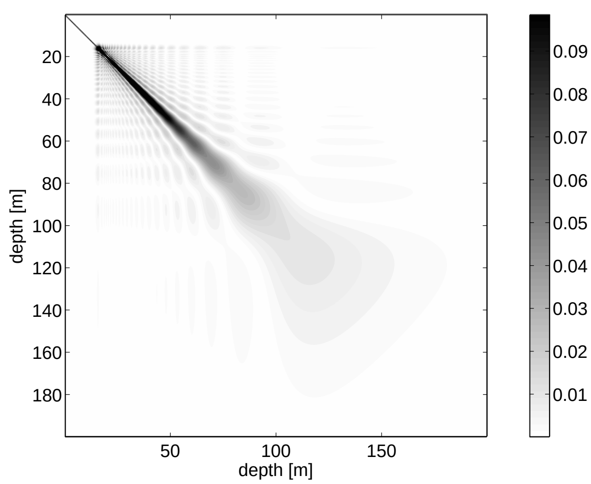

(b)

Figure 1: a) Kernel function of 100 m loop diameter and 100 Ωm homogeneous half space resistivity. b) Model resolution R^m for this kernel function

Λ_p is diagonal and contains the singular values in decreasing order $\lambda_1 \geq ... \geq \lambda_p \geq \lambda_{p+1} = ... = \lambda_q = 0$, $q = min(m,n)$, p rank of A. $U \in \mathbb{C}_1^{n\times n}$ and $V \in \mathbb{C}_2^{m\times m}$ denote unitary [1] matrices formed by the complete set of Eigenvectors of A. The pseudo (or generalized) inverse $A^\dagger$ is then

$$A^\dagger = V_p \Lambda_p^{-1} U_p^T \tag{4}$$

Owing to the ill-posedness of the problem the inverse operator $A^\dagger$ can resolve only $x^{est} = A^\dagger d$ which is not exactly the true subsurface water content because $A^\dagger \neq A^{-1}$. Hence an operator mapping between x and x^{est} describes the difference between the real water content x in the subsurface and the invertible noise free water content x^{est}. For our depth and resolution studies we focus at this model resolution operator R^m

$$\begin{aligned} x^{est} &= A^\dagger y = A^\dagger A x = R^m x && (4)\\ R^m &= A^\dagger A && (5) \end{aligned}$$

or in term of SVD

$$R^m = V_p \Lambda_p^{-1} U_p^T U_p \Lambda_p V_p^T = V_p V_p^T \tag{6}$$

It is obvious that $V\ V^T = V_p V_p^T = \delta_{i,j}$ is valid only for vanishing null-space ($V_0 = empty$) and for this particular case $x^{est} = x$. For every non vanishing null-space R^m acts as a weighting operator

$$x_i^{est} = \sum_{j=1}^{m} R_{i,j}^m x_j \tag{7}$$

[1] A is unitary if and only if $A^{-1} = A^T$

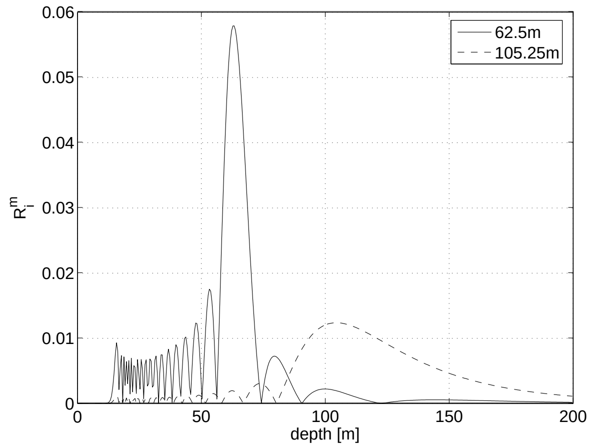

(a)

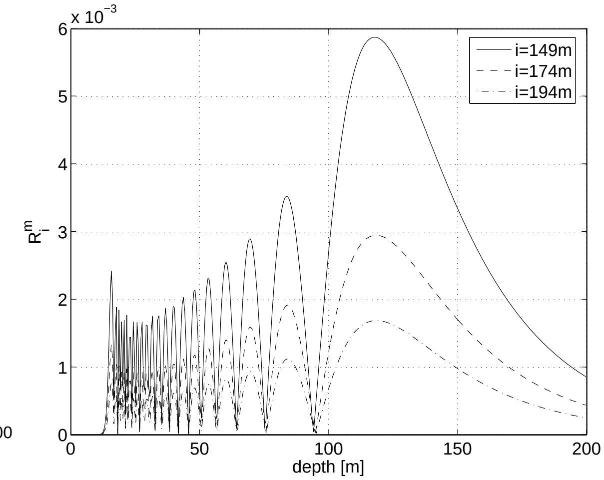

(b)

Figure 2: Slice through model resolution matrix at various depth for calculated kernel function of 100 m loop diameter and 100 Ωm homogeneous half space resistivity. The inverted water content at these depth is a weighted (by the function shown above) average of the complete real water content distribution.

that means every nonzero off-diagonal element of $R^m_{i,j}$ is decreasing model resolution for a specific x^{est}_i because parts of the true water content x are mapped into one single x^{est}_i. Analysing R^m row by row one can achieve detailed information on resolution for every x^{est}_i and furthermore for any depth since the index of x^{est}_i is identified with depth. In Fig. 2 selected rows of R^m are plotted. With decreasing resolution the peak width increases and stronger side lobes appear. Following this interpretation of R^m as weighting operator the resolution (or resolution radius) at any depth can be defined as full width at half maximum for the main peak as long as the maximum of side lobes is small compared to the main peak (Fig. 2 a). For larger depth the increasing influence of side lobes is shown in Fig. 2 b. In this case it is no longer reliable to assign x^{est}_i to a closed part of x (resolution radius), but there is still sensitivity for monitoring changes within deep structures. Thus two different ways are proposed to derive this maximum penetration depth of one specific configuration (loop size and resistivity distribution). First the position of the main peak maximum appears the be constant and can be defined as the maximum penetration depth (Fig. 3 b). Second, as shown above for a vanishing null-space

$$V_p V_p^T = \delta_{ij} \tag{8}$$

and furthermore

$$\sum_{j=1}^{m} R^m_{i,j} = 1 \tag{9}$$

As a result of this (see Fig. 3 a) for any non vanishing null-space

$$\sum_j R^m_{i,j} \leq 1 \;\forall\; j \in [max(peakwidth)\; max(peakwidth)/2] \tag{10}$$

which means for a significant increasing value in Equation 10 the side lobes influence decreases. Both approaches show simular results for the maximum penetration depth.

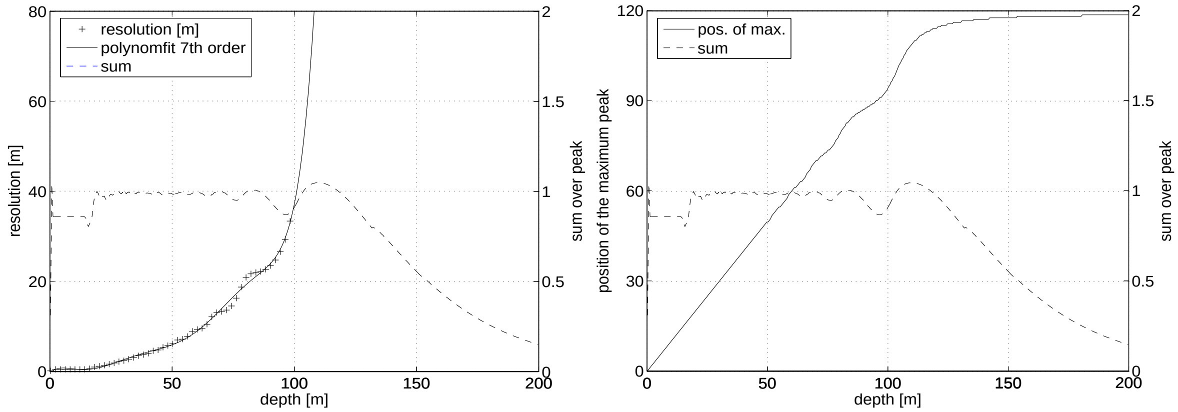

(a) (b)

Figure 3: a) Position of the main peak maximum (main influence to the water content in one specific depth) compared to sum over peak (see eq. 10)
b) Resolution (peak width) and polynomial fit (due to numeric model border effects) compare to sum

Resolution and depth penetration considering noisy conditions Taking real data into account noise has to be included. After triangle inequality in Hilbert space the stability of the solution is directly connected to ill-posedness of the Inverse Problem and the noise level of your data (for detail see [4])

$$||x_n^{est} - x|| \leq ||x_n^{est} - x_n|| + ||x_n - x|| \quad (11)$$

$$\leq ||A_n^\dagger|| * ||y^{est} - y|| + ||A_n^\dagger y - x|| \quad (12)$$

$$||x_n^{est} - x|| \leq ||A_n^\dagger||\delta + ||A_n^\dagger Ax - x|| \quad (13)$$

$$\lim_{n\to\infty} ||A_n^\dagger|| = \infty \quad (14)$$

$$||A_n^\dagger Ax - x|| \overset{n\to\infty}{\longrightarrow} 0 \quad (15)$$

where δ denotes the noise level, y^{est} the noisy data and n the number of singular values taken into account (truncated SVD). Obviously n has to be chosen in a way to satisfy both stability (eq. 14) and approximation of the solution (eq. 15). Furthermore if δ increases n has to be chosen smaller ($n \ll p$) and consequently the model resolution decreases.

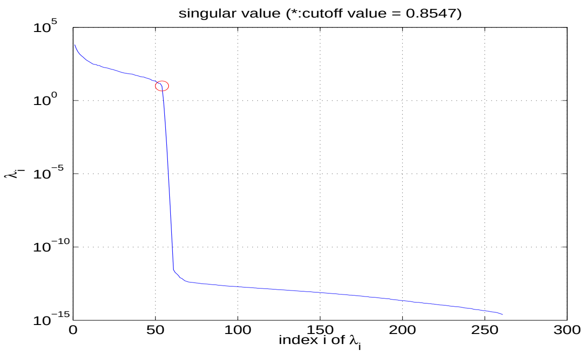

Figure 4:
Spectrum of singular value for calculated kernel function of 100 m loop diameter and 100 Ωm homogeneous half space resistivity. The red circle marks the maximum index of singular values considered for resolution studies.

Conclusion Based on the developed strategies we use the maximum penetration depth and a resolution depth defined as $\frac{1}{10}$ loop diameter resolution radius to evaluate the influence of different loop sizes from 1m to 10000m and resistivities from $1\Omega m$ to $10000\Omega m$ for noise free conditions, therefore $n = p$ can be set (Fig. 4 show the spectrum of singular value). But it has to be remarked that this is the best case scenario and for any other noisy case lower resolution has to be expected. Fig.5 now illustrates the dependency of resolution from loop size and resistivity. One can see that the influence of resistivity increases for increased loop sizes and penetration depth is strongly dependent on resistivity even for small loop sizes. The functional relationship for the penetration depth normalized to loop size appears to be quadratic. Now it can be derived that the MRS technique reaches physical limits of penetration depths in general when considering limited space for very large loops. But since exploration of water saturated layers is one of the basic tasks of MRS, geological relevant resistivities of sedimentary formations have to be taken into account. In this case even large loops seem to be limited to shallow investigations.

References

[1] Martina Braun, Marian Hertrich, and Ugur Yaramanci. Complex inversion of MRS data. *Near Surface Geophysics (accepted)*, 2004.

[2] Sven Friedel. Resolution, stability and efficiency of resistivity tomography estimated from a generalized inverse approach. *Geophysical Journal International*, 153:305–316, 2003.

[3] Marian Hertrich, Martina Braun, and Ugur Yaramanci. Magnetic resonance soundings with separated transmitter and receiver loops. *Near Surface Geophysics*, 3(3):141–154, August 2004.

[4] Bernd Hofmann. *Mathematik inverser Probleme*. B.G. Teubner Stuttgard Leipzig, 1999.

[5] A. Legchenko, Jean-Michel Baltassat, Alain Beauce, and Jean Bernard. Nuclear magnetic resonance as a geophysical tool for hydrogeologists. *Journal of Applied Geophysics*, 50(1-2):21–46, 2002. Special Issue.

[6] A. Legchenko and O. Shushakov. Inversion of surface NMR data. *Geophysics*, 63(1):75–84, 1998.

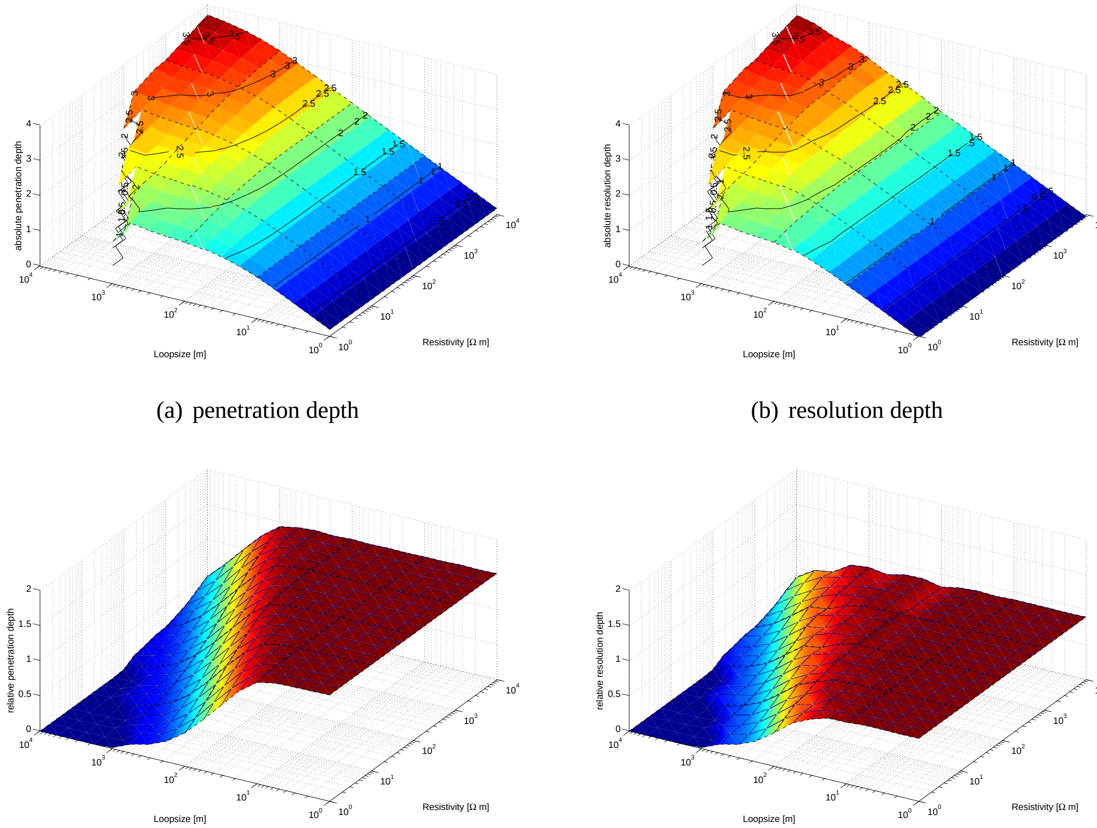

(a) penetration depth

(b) resolution depth

(c) relative penetration depth

(d) relative resolution depth

Figure 5: Influence of different loop sizes and resistivities to maximum penetration and resolution depth where relative means normalized to the loop diameter.